International Journal of Pharmaceutics 426 (2012) 291–301

Contents lists available at SciVerse ScienceDirect

International Journal of Pharmaceutics

journal homepage: www.elsevier.com/locate/ijpharm

Pharmaceutical nanotechnology

# Preparation of E-selectin-targeting nanoparticles and preliminary in vitro evaluation

Emile Jubeli[a], Laurence Moine[a], Valérie Nicolas[b], Gillian Barratt[a,*]

[a] Université Paris-Sud11, Faculté de Pharmacie, 5 rue J.B. Clément CHATENAY-MALABRY, FR 92296, UMR 8612 CNRS, LabEx LERMIT, France
[b] Université Paris-Sud11, Faculté de Pharmacie, 5 rue J.B. Clément CHATENAY-MALABRY, FR 92296, Plateforme d'Imagerie Cellulaire, LabEx LERMIT, France

ARTICLE INFO

*Article history:*
Received 23 November 2011
Received in revised form 11 January 2012
Accepted 13 January 2012
Available online 23 January 2012

*Keywords:*
Carbohydrate ligand conjugated polymers
E-selectin
HUVECs
Nanoparticles

ABSTRACT

Targeted delivery aims to concentrate therapeutic agents at their site of action and thereby enhance treatment and limit side-effects. E-selectin on endothelial cells is markedly up-regulated by cytokine stimulation of inflamed and some tumoral tissues, promoting the adhesion of leukocytes and metastatic tumor cells, thus making it an interesting molecular target for drug delivery systems.

We report here the preparation of targeted nanoparticles from original amphiphilic block copolymers functionalized with an analog of sialyl Lewis X (SLEx), the physiological ligand of E-selectin. Nanoparticles, prepared by nanoprecipitation, caused no significant cytotoxicity. Ligand-functionalized nanoparticles were specifically recognized and internalized better by tumor necrosis factor α (TNF-α)-activated human umbilical vein endothelial cells (HUVECs) than control nanoparticles or HUVECs with low E-selectin expression. These nanoparticles are designed to carry the ligand at the end of a PEG spacer to improve accessibility. This system has potential for the treatment of inflammation, inhibition of tumor metastasis, and for molecular imaging.



## 1. Introduction

The use of colloidal carriers is a promising strategy to achieve controlled release and/or site specific targeting of a drug after intravenous administration. However, a successful formulation must have a carefully designed chemical structure and surface properties. One of the major prerequisites for colloidal particles for intravenous administration is to have a hydrophilic surface in order to avoid rapid elimination from the blood stream by the macrophages of the mononuclear phagocyte system and the consequent accumulation of the delivery system in the liver and the spleen (Brigger et al., 2002). This can be achieved by grafting hydrophilic flexible chains of poly (ethylene glycol) (Gref et al., 1997, 2001) or polysaccharides (Chauvierre et al., 2003; Passirani et al., 1998) onto their surface.

In an attempt to modify the passive distribution of nanoparticles and their drug cargo, specific ligands able to recognize molecules overexpressed or exclusively present on the target cells, tissues or organs can be grafted to the surface of the carriers. Ligands that have been tested for this purpose include antibodies (Bendas et al., 1999; Everts et al., 2003), antibody fragments (Kang et al., 2002a,b), peptides (Myrset et al., 2011; Shamay et al., 2009; Zhang et al., 2008) and folic acid (Stella et al., 2007; Wang et al., 2011).

Among the possible targets for this approach are the selectins, a family of three calcium-dependent transmembrane glycoproteins. E-selectin, also known as ELAM-1, is markedly up-regulated in endothelial cells when they are activated by proinflammatory factors such as TNF-α (tumor necrosis factor alpha), interleukin-1 (IL-1) and bacterial lipopolysaccharide (LPS) (Bevilacqua et al., 1989; Montgomery et al., 1991). Once expressed on the surface of cell, it is efficiently internalized by endocytosis (von Asmuth et al., 1992). E-selectin specifically recognizes the tetrasaccharide sialyl Lewis X (SLEx), the terminal epitope of the structure of glycoproteins and glycolipids located on the surface of leukocytes and tumor cells (Phillips et al., 1990; Walz et al., 1990). The E-selectin-SLEx interaction via weak bonds initiates leukocyte "rolling", the first step in leukocyte adhesion and infiltration into tissues undergoing inflammation, cancer or ischemic stress. Therefore, E-selectin is a very interesting target for the site-specific delivery of colloidal drug delivery systems.

Some reports have been published in which drug carriers have been directed toward this receptor by means of anti-E-selectin antibodies (Asgeirsdottir et al., 2008; Pattillo et al., 2009), but this strategy is hampered by possible immunogenicity, the large size of the final delivery system and the high cost of antibody production. A further disadvantage of antibodies is that they may have restricted species specificity, i.e. they may be active in animal models but do

* Corresponding author. Tel.: +33 01 46 83 56 27; fax: +33 1 46 83 59 46.
*E-mail address:* gillian.barratt@u-psud.fr (G. Barratt).

0378-5173/$ – see front matter © 2012 Elsevier B.V. All rights reserved.
doi:10.1016/j.ijpharm.2012.01.029

not cross-react with the human epitope. Another approach to targeting E-selectin is the use of its physiological ligand SLEx coupled to drug carriers such as liposomes (Minaguchi et al., 2008; Stahn et al., 2001) or nanoparticles (van Kasteren et al., 2009). However, as well as the complex and expensive synthesis of this ligand, and its instability, these drug delivery systems could be in competition with SLEx found on leukocytes that would also be concentrated in the targeted region because of chemotaxis.

A way to overcome these problems is to use small saccharide-based ligands with a simple structure that would be non-immunogenic and recognize E-selectin with a higher affinity than its natural ligand. Recent advances in glycobiology and carbohydrate derivative chemistry have allowed several high-affinity analogs mimicking SLEx to be developed. The most frequently used strategy has been the substitution of the sugars in SLEx and/or the introduction of secondary groups while ensuring that the key interactions with E-selectin were retained. The analogs described in the literature have diverse structures based mono, bi, tri or tetrasaccharide derivatives or even molecules whose structures are not based on SLEx (Kaila and Thomas, 2002; Simanek et al., 1998). The group of Wong has been very active in the field and have synthesized a small mannose-based SLEx analog (Wong et al., 1997) with five times higher affinity for E-selectin than native SLEx in a cell-free test (Weitz-Schmidt et al., 1996). Moreover, it has been successfully used as a recognition element when coupled directly to a nanoparticle surface via a glycidyl ether linkage without a spacer (Banquy et al., 2008). Therefore, this molecule was an ideal ligand to evaluate our original macromolecular strategy to construct a delivery system targeting selectin.

Among the biocompatible polymers that have been used to manufacture colloidal drug delivery systems, poly(lactic acid-co-glycolic acid) (PLGA) and its block copolymer with poly(ethylene glycol) (PEG-PLGA) have been by far the most widely used, particularly since they are commercially available. However, it is not possible to modulate the composition of these preformed polymers in order to adjust their physico-chemical properties (solubility, degradation) for particular applications. Furthermore, their chemical structure (with only one hydroxyl group per chain) limits their capacity to carry attached ligands since it is difficult to modulate the number and position of the ligands on the particle surface. Over the past decade, spectacular advances in polymer synthesis have paved the way to obtaining macromolecular architecture with controlled molecular weight, narrow molecular weight distribution and high degree of functionalization. Thus, several routes of controlled radical polymerization and efficient coupling methods have emerged. In particular, the Cu(I)-catalyzed azide-alkyne cycloaddition, the most efficient among the "click" reactions, can be carried out under simple reaction conditions in organic to aqueous solvents with high yields (Hartmuth et al., 2001).

In a previous article, we reported the synthesis of an amphiphilic block copolymer bearing a monosaccharide as a model of a carbohydrate ligand on its hydrophilic part (Jubeli et al., 2010). This polymer could be used to prepare nanoparticles using a simple nanoprecipitation method, without any surfactant. These nanoparticles did not display significant cytotoxicity to endothelial cells and the accessibility of glucopyranoside molecules on their surface was confirmed by formation of aggregates in the presence of the lectin Concanavalin A.

This macromolecular strategy offers many advantages. Firstly, the ligand is separated from the hydrophobic core of the particles by a flexible PEG spacer that has the double role of rendering the surface hydrophilic and increasing the accessibility of the ligand. Indeed, the positioning of a ligand at the end of the PEG chain has often been observed to be more effective than direct coupling to the surface of the carrier (Bendas et al., 1999; Zeisig et al., 2004). Ligand conjugation to the end of PEG chains can be carried out by "click chemistry", as described above. Secondly, the connection of PEG chains with the hydrophobic block of poly (D,L-lactide) (PLA) is achieved via a methacrylate block where each unit bears a PEG side-chain terminated by a ligand. Unlike the commonly used PEG-PLGA diblock copolymer, this novel structure synthesized from a macromonomer of PEG carries several grafted functionalized hydrophilic pendant chains. In this way, the amount of ligand at the surface can be controlled by varying the initial percentage of introduced macromonomer. Moreover, it is well documented that the presence of many copies of pendant saccharides on a polymer backbone can enhance their affinity toward cell-surface lectins because of multivalent recognition, known as the "cluster effect" (Lee and Lee, 1995; Lundquist and Toone, 2002).

Based on this preliminary work, glucose was replaced by the mannose based analog of SLEx mentioned above (Wong et al., 1997) to prepare a polymer able to specifically recognize E-selectin. With this novel copolymer, our goal was to mimic the interaction of leukocyte/endothelial cells by designing biodegradable polymeric nanoparticles with fully controllable properties that could target endothelial cells with up-regulated E-selectin expression. Since this receptor is implicated in inflammatory pathologies diseases such as rheumatoid arthritis (Kriegsmann et al., 1995; Wikaningrum et al., 1998), liver inflammation (Adams et al., 1996), autoimmune uveoretinitis (Hashida et al., 2008), and also some cancers where E-selectin is present on the vasculature of tumor tissue; for example, human colorectal cancer (Kiriyama and Ye, 1995), gastric cancer (Mayer et al., 1998) head and neck (Renkonen et al., 1999) or breast tumors (Nguyen et al., 1997), the therapeutic potential of such nanoparticles would be high.

In this work, we report the synthesis of the glycopolymer, the preparation of nanoparticles, their characterization, in vitro cytotoxicity and in vitro interactions with activated endothelial cells. Fluorescent nanoparticles were prepared from a fluorescently labeled copolymer. Their association with endothelial cells was evaluated qualitatively through observation by confocal microscopy and quantitatively by measuring cell-associated fluorescence by spectrofluorimetry.

## 2. Materials and methods

### 2.1. Chemicals

Poly(ethylene glycol) methacrylate PEGMA (Mn ≈ 526 g/mol), poly(ethylene glycol) methyl ether methacrylate (300 g/mol), tin (II) 2-ethylhexanoate ($Sn(Oct)_2$ 95%) and N,N′,dicyclohexyl carbodiimide (DCC 99%), 3-[4,5-dimethylthiazol-2-yl]-2,5-diphenyltetrazolium bromide were purchased from Sigma–Aldrich. 2-Bromo-2-methylpropionyl bromide (98%) and N,N,N′,N″,N″-pentamethyldiethylenetriamine (PMDETA) were obtained from Acrôs organics (Belgium). Trimethylamine (99.5%) and 4-pentynoic acid 98% were purchased from Alfa Aesar-UK. Methacryloxyethyl thiocarbamoyl rhodamine B and D,L-lactide were purchased from Biovalley. Palladium hydroxide 20% on carbon was obtained from TCI. Copper (I) bromide (Cu(I)Br) (Sigma–Aldrich) was washed with glacial acetic acid, filtered, washed with ethanol and dried under vacuum. PEGMA was purified before use as described previously(Ali and Stover, 2004). Dibenzyl N-[(6-azido-6-deoxy-2,3,4-tri-O-benzyle-α-D-mannopyranosyl)]-L-glutamic acid (referred to as Man-glu in the text) was synthesized by Symphabase (Switzerland).

For the synthesis and characterization of the bifunctional initiator, PLA-PEGMA (7) and PLA-PEGMMA-Rhodamine (8) see the Supporting Information.

### 2.2. Instruments

$^1$H-NMR measurements were performed with a Bruker 300 MHz spectrometer. Size exclusion chromatography was performed with a double detector: 270 dual viscosimeter and light scattering detector 90° (Viscotek® – France) and a refractometer (Waters® 410). THF was used as the mobile phase with a TOSOH BIOSCIENCE TSKgel 5 μm bead size Guard pre-column; and two TOSOH BIOSCIENCE TSKgel 5 μm bead size GMHHR-M columns, operated at 1 ml/min with the column temperature set at 30 °C. Omnisec® software (Viscotek) was used to process the data.

The mean hydrodynamic diameter and polydispersity of the nanoparticles were measured by quasi-elastic light scattering with a Zetasizer NanoZS90 (Malvern Instruments). Each type of nanoparticle was prepared in triplicate and three measurements were performed for each sample, at a temperature of 25 °C with a detection angle of 90°. Nanoparticle surface charge was investigated by $\zeta$-potential measurement at 25 °C after dilution with 1 mM NaCl.

The fluorescence properties of the nanoparticles were evaluated using a Perkin-Elmer LS50B spectrofluorometer with a 10 mm optical quartz cuvette.

Confocal laser scanning microscopy (Zeiss LSM-510, Carl Zeiss, Germany) was used for in vitro imaging studies. All images were acquired with an air-cooled ion laser at 488 nm (FITC) and 543 nm (rhodamine), performed using Plan Apochromat 63 × /1.4NA oil objective lens. Fluorescence was collected by using a 505–550 nm band pass filter for FITC and a long pass filter beginning at 560 nm for rhodamine. The autofluorescence of HUVECs was found to be negligible under the acquisition settings and did not interfere with the fluorescence coming from the nanoparticles.

### 2.3. Synthesis of acetylene-terminated PEGMA (Pentynoate-PEGMA) (**3**)

An acetylene group was conjugated with PEGMA as described in our previous work (Jubeli et al., 2010). Briefly PEGMA (7.5 g; 14.3 mmol), 4-pentynoic acid (2.8 g; 28.5 mmol) and DMAP (0.17 g; 1.4 mmol) were put in a schlenk tube with 35 ml of methylene chloride ($CH_2Cl_2$). DCC (5.6 g; 27.2 mmol) was solubilized in 5 ml of $CH_2Cl_2$ and then added to the schlenk tube. The mixture was stirred overnight at room temperature. After elimination of dicyclohexylurea (DCU) crystals by filtration, the organic solvent was evaporated under reduced pressure. The resulting yellow oil-like product was purified by column chromatography with a mixture of ethyl acetate/methanol (9:1) as eluant to yield the acetylene-terminated PEGMA (yield = 82%).

$^1$H-NMR (300 MHz, $CDCl_3$, $\delta$ ppm): 1.92 (3H, $CH_2$=C–C**H**$_3$), 1.96 (1H, ≡C**H**), 2.50 (2H, –C**H**$_2$–$CH_2$–C≡CH), 2.51 (2H, –$CH_2$–C**H**$_2$–C≡CH), 3.65 (36H, –C**H**$_2$–, PEG), 4.26 (4H, 2*x* –C**H**$_2$–COO), 5.55 (1H, –**H**HC=C), 6.10 (1H, –H**H**C=C). IR ($cm^{-1}$): 3260 (–C≡CH), 2870 (alkyl), 1620 (–C=C–).

### 2.4. Synthesis of PEGMA-Man-glu-Bz (**4**)

Acetylene-terminated PEGMA (**3**) (0.3 g; 0.5 mmol), Man-glu-Bz (0.62 g; 0.75 mmol), CuBr (0.071 g; 0.5 mmol) and PMDETA (0.086 mg; 0.5 mmol) were introduced in a schlenck tube with 4 ml of DMF. The mixture was stirred for 3 h at room temperature, the reaction was stopped and the content was diluted with ethyl acetate before being submitted to column chromatography using gradient mixtures of cyclohexane/ethyl acetate then ethyl acetate/methanol. The resulting PEGMA-Man-glu-Bz (**4**) was dried under vacuum (yield = 55%).

$^1$H-NMR (300 MHz, $(CD_3)_2O$, $\delta$ ppm): 1.79 (3H, $CH_2$=C–C**H**$_3$), 2.10 (1H, C**H**H–CO–NH–), 2.52 (2H, –$CH_2$–C**H**$_2$–COO), 2.65 (CH, –C**H**$_2$–$CH_2$–C=CH), 2.95 (2H, –$CH_2$–C**H**$_2$–C=CH), 3.62 (36H, –C**H**$_2$–C**H**$_2$ of PEG + 3H –C**H**– mannose ring), 3.80–4.15 (1H, O–C**H**–$CH_2$, mannose ring), 4.15–4.32 (4H, 2*x* –C**H**$_2$–COO), 4.52–4.80 (6H, –C**H**$_2$–Bz, protecting mannose hydroxyl groups), 5.08–5.20 (4H, –C**H**$_2$–Bz, protecting glutamate carboxyl groups), 5.65 (1H, **H**HC=CH–, vinyl), 6.08 (1H, H**H**C=CH vinyl), 7.2–7.45 (25H, aromatic protons), 7.80 (1H, –C=C**H**–N triazole ring). IR ($cm^{-1}$): 3650 (–NH–), 2870 (alkyl), 1720 (–C=O–), 1640 (–C=C), 700 (aromatic C–H).

### 2.5. Synthesis of the PLA macroinitiator (**1**)

D,L-Lactide (8.64 g; 60 mmol), $Sn(Oct)_2$ (10.4 mg; 0.013 mmol) and the synthesized bifunctional initiator β-hydroxyl ethyl α-bromoisobutyrate (HEBIB) (30 mg; 0.28 mmol) were introduced in a schlenk tube and the mixture was bubbled with nitrogen for 30 min. The schlenk tube was placed in a thermostated oil bath at 130 °C and stirred for 6 h. The resulting solid crude product was solubilized with chloroform, and precipitated in a cold mixture of 1:1 petroleum ether/diethyl ether and dried in a vacuum oven at 40 °C to give a white solid (yield 92%). $^1$H-NMR (300 MHz, $CDCl_3$, $\delta$ ppm): 1.55 (3H, C**H**$_3$), 5.2 (1H, –C**H** main chain). $Mn_{NMR}$ = 29,700, $Mn_{SEC}$ = 28,500, $Mw/Mn$ = 1.02.

### 2.6. Synthesis of PLA-block-PEGMA-Man-glu-Bz (**5**) by ATRP

PLA (**1**) (0.320 g; 0.01 mmol), PEGMA-Man-glu-Bz (**3**) (0.311 mg; 0.22 mmol), CuBr (3.1 mg; 0.02 mmol), PMDETA (3.8 mg; 0.02 mmol) were introduced to a schlenk tube with 1 ml of DMSO. After three freeze-pump-thaws, the schlenk tube was placed in a thermostated oil bath at 60 °C and stirred for 24 h. The content was then purified by column chromatography with $CH_2Cl_2$/methanol (9:1) to remove the copper complex. After evaporation of solvents, product (**5**) was dried in a vacuum oven at 45 °C for 48 h, (yield 78%).

$^1$H-NMR (300 MHz, DMSO, $\delta$ ppm): 0.7–1.3 (–C**H**$_2$– main chain of PEGMA), 1.35–1.65 (3H, –C**H**$_3$ PLA), 1.95 (1H, C**H**H–CO–NH–), 2.40 (4H, –C**H**$_2$– C**H**$_2$–COO + 2H –C**H**$_2$–$CH_2$–C=CH), 2.8 (2H, –$CH_2$–C**H**$_2$–C=CH), 3.20–3.70 (36H, –C**H**$_2$– of PEG + 4H, –C**H**– mannose ring and), 4.14 (4H, 2*x* –C**H**$_2$–COO), 4.32–4.72 (6H, –C**H**$_2$–Bz, protecting mannose hydroxyl groups), 4.9–5.30 (4H, –C**H**$_2$–Bz, protecting glutamate carboxyl groups + 1H, –C**H**– main chain of PLA), 7.15–7.4 (25H, aromatic protons), 7.7 (1H, –C=C**H**–N triazole ring). IR ($cm^{-1}$): 3650 (–NH–), 2870 (alkyl), 1720 (–C=O–), 700 (aromatic C–H). $Mn_{NMR}$ = 44,700, $Mn_{SEC}$ = 38,200 and $Mw/Mn$ = 1.09.

### 2.7. Deprotected PLA-block-PEGMA-Man-glu-OH (**6**)

The benzyl groups protecting the three hydroxyl groups of mannose and the two carboxyl groups of glutamate in the structure of Man-glu-Bz were reduced by catalytic debenzylation in the presence of hydrogen gas. Product (**5**) (0.450 g) was dissolved in a 10 ml mixture of THF: glacial acetic acid (1:4) in a cylindrical tube, then 400 mg of palladium hydroxide 20% on carbon was dispersed in the solution. After degassing with argon for 10 min, the tube was introduced to a special cell, filled with hydrogen gas and maintained under a pressure of 6 bars. The mixture was stirred vigorously with a magnetic stirrer for 72 h. After filtration through celite to remove the palladium-carbon, solvents were evaporated under vacuum at 45 °C; the deprotected product (**6**) was obtained with a 91% yield. $^1$H-NMR (300 MHz, $(CD_3)_2CO$, $\delta$ ppm): 0.8–1.3 (–C**H**$_2$– main chain of PEGMA), 1.45–1.70 (3H, –C**H**$_3$ PLA), 2.25 (1H, C**H**H–CO–NH–), 2.60 (4H, –C**H**$_2$– C**H**$_2$–COO + 2H –C**H**$_2$–$CH_2$–C=CH), 3.00 (2H, –$CH_2$–C**H**$_2$–C=CH), 3.50–3.78 (36H, –C**H**$_2$– of PEG + 4H,–C**H**– mannose ring), 4.14–4.42 (4H, 2*x* –C**H**$_2$–COO), 5.15–5.38 (1H,

—C**H**— main chain of PLA), 7.33 (1H, —C=C**H**—N triazole ring). IR ($cm^{-1}$): 3000–3600 (—OH—), 2870 (alkyl), 1720 (—C=O—).

### 2.8. Preparation of nanoparticles

Nanoparticles were prepared by nanoprecipitation. 10 mg of a 1:1 mixture of PLA-PEGMA-Rhod (**8**) and PLA-PEGMMA (**7**) or PLA-PEGMA-Man-glu-OH (**6**) were dissolved in 2 ml of DMF. This solution was added dropwise to 4 ml of water under moderate stirring through a needle (0.8 mm internal diameter) over 1 min. The crude nanoparticle suspension was centrifuged (Centrifuge Eppendorf 5804 R) at $4500 \times g$ for 10 min at 20 °C to separate larger polymer aggregates from nanoparticles that remained in the supernatant, then DMF was removed by 4 h dialysis (MWCO 15,000 Da) against deionized water.

### 2.9. Fluorescent properties of labeled copolymer and nanoparticles

The fluorescent properties of copolymer (**8**) and nanoparticles containing this copolymer were studied by fluorescence spectroscopy. Excitation and emission wavelengths were determined for a solution (5 mg/ml) of copolymer (**8**) in THF and for a suspension of nanoparticles in water (5 mg/ml) prepared from a 1:1 mixture of copolymers (**7** and **8**). Calibration curves of fluorescence emission intensity as a function of the concentration of polymers in THF and of nanoparticles in water were drawn in the range of 0.01–1 mg/ml.

### 2.10. Cell culture and viability assay

Freshly isolated human umbilical vein endothelial cells (HUVECs) (Hospital Bichat – Paris, France), were cultured in Endothelial Cell Growth Medium (Promocell – Germany) supplemented with 2% fetal calf serum (FCS), 0.1 ng/ml epidermal growth factor, 1 ng/ml basic fibroblast growth factor, 90 μg/ml heparin, 1 μg/ml hydrocortisone, 50 U/ml penicillin, and 50 μg/ml streptomycin. Cells were maintained at 37 °C under a humidified atmosphere containing 5% $CO_2$.

The cytotoxicity of nanoparticles was estimated by assessing cell viability on HUVECs using the 3-[4,5-dimethylthiazol-2-yl]-2,5-diphenyltetrazolium bromide (MTT) assay measuring mitochondrial dehydrogenase cell activity. Cells were seeded in the above mentioned medium into 96-well plates at a density of $10^4$ cells/well. After an adherence period of 24 h, different dilutions of nanoparticles (0.05–0.5 mg polymer/ml of culture medium) were added to the cells. Each dilution was tested in at least 5 wells. After 48 h of incubation at 37 °C, 20 μl of MTT (Sigma–Aldrich, Saint Quentin Fallavier, France) in PBS (5 mg/ml) were added to each well. After further incubation for 2 h at 37 °C, culture medium was removed and formazan crystals were dissolved in 200 μl DMSO. The absorbance of converted dye, an indication of the number of viable cells, was measured at 570 nm using a microplate reader (Labsystems multiscan MS). The percentage of cell viability was calculated as the absorbance ratio of treated to untreated cells.

### 2.11. Immunodetection of E-selectin

HUVEC cells were seeded on sterile round coverslips at a density of $5 \times 10^4$ cells/well into 24-well plates and grown for 48 h prior to activation by 50 ng/ml of recombinant human TNF-α (R&D systems) for 4 h. After rinsing with PBS, cells were fixed with 4% solution of paraformaldehyde (Sigma–Aldrich), then free aldehyde groups were quenched with 50 mM solution $NH_4Cl$ in PBS. Non-specific sites were blocked with 5% bovine serum albumin solution (BSA – Sigma–Aldrich). Cells were then incubated overnight at 4 °C with monoclonal anti-human E-selectin antibody (R&D systems) (10 μg/ml in 5% BSA). After washing with PBS, cells were incubated for 2 h with a 1:300 dilution of secondary anti-mouse Alexa 546-labeled antibody (Invitrogen). In order to stain cell lipids and particularly the cell membrane, cells were incubated with a 100 μl solution (2:100) in PBS of FITC-PKH67 fluorescent dye (Sigma–Aldrich). Imaging was carried out with the laser scanning confocal microscope as described above.

### 2.12. Observation and quantification of nanoparticle association with HUVEC

HUVECs were seeded in 24-well plates and activated as described above. Fluorescent nanoparticles (100 μg/well) with or without ligand were incubated with cells for 0.5, 2 and 21 h in 37 °C or 4 °C. For laser scanning confocal microscope observation, cells were fixed with 4% paraformaldehyde as described above after elimination of non associated nanoparticles by repeating washing with PBS.

For quantification of nanoparticle association with cells, the monolayer was lysed with 1 ml of 0.2% Triton X-100 in 1 M NaOH. The nanoparticle content was quantified by spectrofluorometry ($\lambda_{ex}$ = 560 nm, $\lambda_{em}$ = 580 nm). HUVECs incubated with known concentrations of nanoparticles were lysed in 1 ml of 0.2% Triton X-100 in 1 M NaOH and these lysats were used to calibrate the spectrofluorimeter. Linear calibration curves were obtained for nanoparticles with and without ligand ($r$ = 0.9993 and 0.9997 respectively), over a nanoparticle concentration range of 2–100 μg/ml. This linear calibration confirmed that the autofluorescence of HUVECs was negligible and did not interfere with nanoparticle fluorescence under our experimental conditions.

To determine the specificity of E-selectin binding, a similar procedure was used in which the cells were preincubated with a monoclonal anti-human E-selectin antibody (10 μg/ml) for 1 h before determining the association of nanoparticles.

## 3. Results

During the early stages of our work, we successfully synthesized an amphiphilic copolymer with block architecture decorated on its hydrophilic part with a monosaccharide as a model of a carbohydrate ligand (Jubeli et al., 2010). The glucopyranoside used was first coupled with a poly (ethylene glycol) methacrylate macromonomer by "click chemistry". Thereafter, the construction of the copolymer was carried out by a combination of two types of polymerization: ATRP (Atom Transfer Radical Polymerization) for the hydrophilic part and ROP (Ring Opening Polymerization) for the hydrophobic part. The presence of glucopyranoside residues on the surface of nanoparticles formed from this copolymer was demonstrated through their interactions with Concanavalin A.

In the present work, we have extended our methodology to the preparation of particles carrying a SLEx analog in place of monosaccharide in order to study their ability to mimic the interactions between leukocytes and activated endothelial cells. Our choice was to use a mannose-based SLEx analog, synthesized for the first time by Wong et al. (Wong et al., 1997), because of its simple structure and its moderate cost as well as its high affinity for E-selectin (Weitz-Schmidt et al., 1996). The properties of this analog would make these nanoparticles a very interesting candidate for a drug delivery system targeting E-selectin.

### 3.1. Synthesis of PEGMA-Man-glu-Bz (*4*)

The preparation of the ligand-functionalized macromonomer was carried out by click chemistry. PEGMA was first reacted

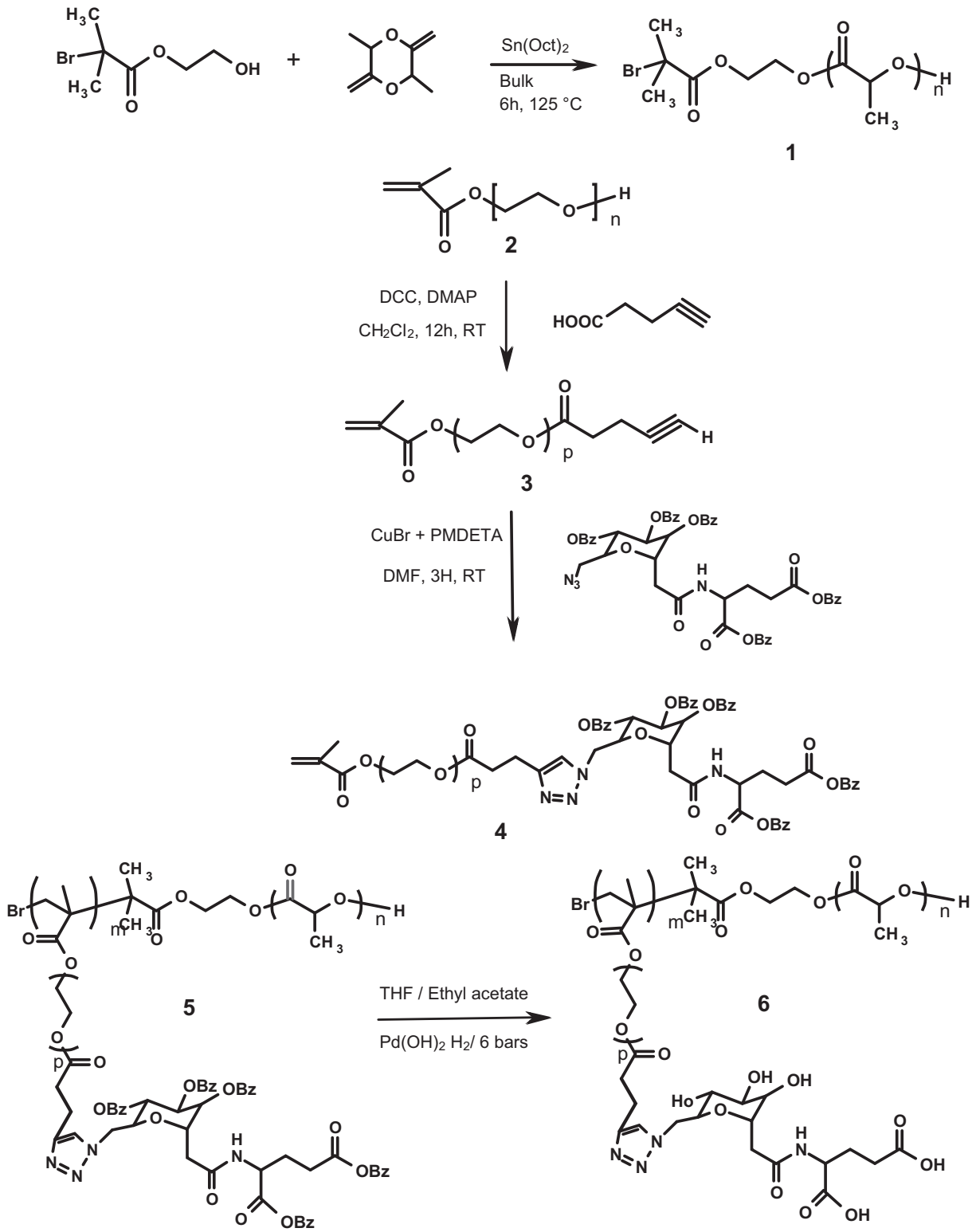


**Fig. 1.** Synthesis of the amphiphilic copolymer.

with 4-pentynoic acid by an esterification reaction leading to the alkyne-terminated PEGMA (**3**) (Fig. 1). Thereafter, N-[(6-deoxy-6 azido α-D-Mannopyranosyl)]-L-glutamic acid (Man-glu) was introduced by Cu-catalyzed [2 + 3] cycloaddition to provide the macromonomer (**4**). The time of this reaction was fixed at 3 h, leading to a high conversion ratio while maintaining the integrity of methacrylate double bond (Fig. 2).

### 3.2. Synthesis of amphiphilic copolymers

In order to evaluate this nanoparticulate system, we synthesized different copolymers including a ligand-functionalized copolymer (**6**), a non functionalized copolymer (**7**) and fluorescent copolymer (**8**). Different combinations of these were used to prepare nanoparticles in order to study their in vitro interaction with cells.

**Table 1**
quantified by spectrofluorometry ers.

| | Polymer | M/I | % conv NMR | Mn Theo | Mn NMR | Mn SEC | PDI *Mw*/*Mn* |
|---|---|---|---|---|---|---|---|
| **1** | PLA | 1/420 | 92 | 30,200 | 29,700[a] | 28,500 | 1.05 |
| **5** | PLA-PEGMA-Man-glu-Bz | 1/20 | 80 | 57,600 | 44,700[b] | 38,200 | 1.10 |
| **6** | PLA-PEGMA-Man-glu-OH | – | – | 42,000 | 35,500[c] | ND | ND |
| **7** | PLA-PEGMMA | 1/20 | 89 | 35,000 | 36,000[d] | 44,600 | 1.14 |
| **8** | PLA-PEGMMA-Rhod | 1/20 | 72 | 31,000 | 28,000[d] | 28,900 | 1.12 |

[a] Calculated from the relative integration values of the main chain (—CH—) of PLA and the two (—$CH_3$—) of the initiator.
[b] Calculated from the relative integration values of the main chain (—CH—) of PLA and the (—CH—) of triazole ring.
[c] Calculated from the relative integration values of the main chain (—CH—) of PLA and the (—$CH_2$—) of PEG chain.
[d] Calculated from the relative integration values of the main chain (—CH—) of PLA and the (—$OCH_3$) of PEGMMA.

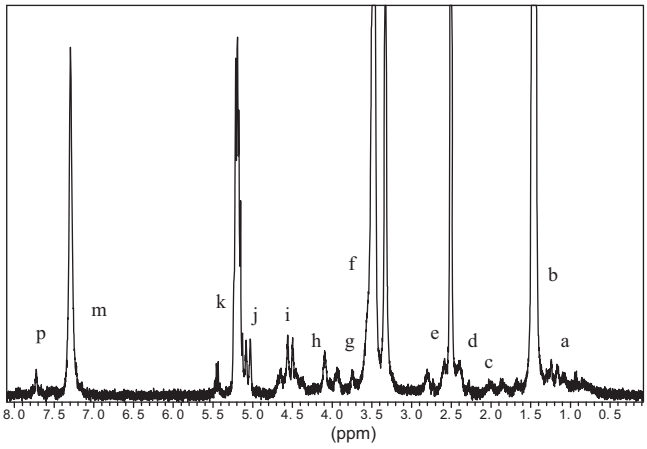


**Fig. 2.** $^1$H-NMR spectrum of PLA-PEGMA-Man-glu-Bz (**5**).

For the synthesis of copolymers (**7**) and (**8**), we were guided by our previous work using anisole as solvent. However, our first attempts at ATRP polymerization with the ligand-based PEGMA monomer in anisole resulted in a very low conversion rate according to $^1$H-NMR (<30%). Although DMSO is rarely used in the preparation of polymers, it is quite efficient at dissolving the PLA and ligand-functionalized pegylated monomer, thus its use allowed us to obtain a conversion rate of more than 75% (Table 1) keeping CuBr/PMDETA complex as catalyst but with a longer polymerization time of 24 h (Wolf et al., 2009).

Pendant benzyl groups were removed by catalytic hydrogenolysis using severe conditions (6 bars pressure, 72 h, and high amount of palladium). Milder conditions were not sufficient to achieve deprotection. Details of the synthesis and characterization ($^1$H-NMR, SEC and IR analyses) of the different polymers are available as supplementary data.

### 3.3. Characterization of nanoparticles

Nanoparticles were prepared in a single step by nanoprecipitation. Nanoparticles both with and without ligand (Fig. 3) showed a homogeneous mean diameter of around 170 nm with a unimodal size distribution (Table 2). After two weeks of storage at 4 °C in water, no significant size change was detected and no aggregation was observed.

**Table 2**
Properties of nanoparticles prepared with and without ligand.

| | Copolymers | Size (nm) | PDI[a] | Zeta potential (mV) |
|---|---|---|---|---|
| NP-Ligand-Rhod | (**6**+**8**) | 178 ± 10.9 | 0.167 | −21.9 |
| NP-Rhod | (**7**+**8**) | 165 ± 1.6 | 0.124 | −28.4 |

[a] Polydispersity index

Negative zeta potential values were observed for both types of nanoparticles, due to the end groups of PLA block of the copolymer, even in the presence of PEG chains. It has been reported that a high PEG weight content is needed to completely mask the charge of PLA (Gref et al., 2000); however the nanoparticles prepared in this study had quite short PEG chains. The slightly more negative values obtained for Man-glu-OH carrying nanoparticles could be attributed to the two carboxylic groups present in the ligand.

### 3.4. Characterization of fluorescently labeled copolymer and nanoparticles

The fluorescence spectra of a solution of the rhodamine-substituted polymer (**8**) in THF were studied. The excitation and emission maxima wavelengths were found to be $\lambda_{ex}$ = 559.5 nm and $\lambda_{em}$ = 580.5 nm (Fig. S7) which are in agreement with results obtained with other rhodamine-labeled polymers in solution (Brambilla et al., 2010).

Similar values were observed for a 5 mg/ml suspension of nanoparticles prepared from a 1:1 mixture of copolymers (**7**) and (**8**): $\lambda_{ex}$ = 560 nm and $\lambda_{em}$ = 579 nm (Fig. S8). A linear relationship between the fluorescence intensity and concentration were observed for polymer in THF (0.01–1 mg/ml $R^2$ = 0.9993) and for nanoparticles in water (0.01–0.8 mg/ml $R^2$ = 0.9997).

### 3.5. Cell viability studies

The impact of fluorescent nanoparticles prepared with and without the ligand was determined on freshly isolated HUVECs after 48 h of incubation at 37 °C using the MTT test. The results reported in Fig. 2 show cell viability higher than 60% in the range of (0–500 μg/ml), for both types of fluorescent nanoparticles.

Nanoparticles prepared only from copolymer (**7**) (without rhodamine) were also tested to distinguish any additional toxicity of the rhodamine incorporated in the polymer backbone. It is evident from Fig. 2 that rhodamine-containing nanoparticles have an identical effect on cell viability to that of non-fluorescent nanoparticles.

In the light of these results, we chose a concentration of 100 μg/ml of nanoparticles, at which cell viability was higher than 80%, for the evaluation of nanoparticle association with HUVEC cells (Fig. 4).

### 3.6. Immunodetection of E-selectin

HUVECs were used as an endothelial cell model because of their human origin, and also because they are well characterized, widely used to investigate vascular events in vitro, and can be treated with cytokines to generate an in vitro model of activated endothelium.

Pro-inflammatory TNF-α-activated HUVECs and non activated HUVECs were incubated with anti-human E-selectin antibody and examined by confocal microscopy in order to detect the basal and stimulated expression of the receptor. Activated cells were fixed 4 h after incubation with TNF-α as it was reported that E-selectin

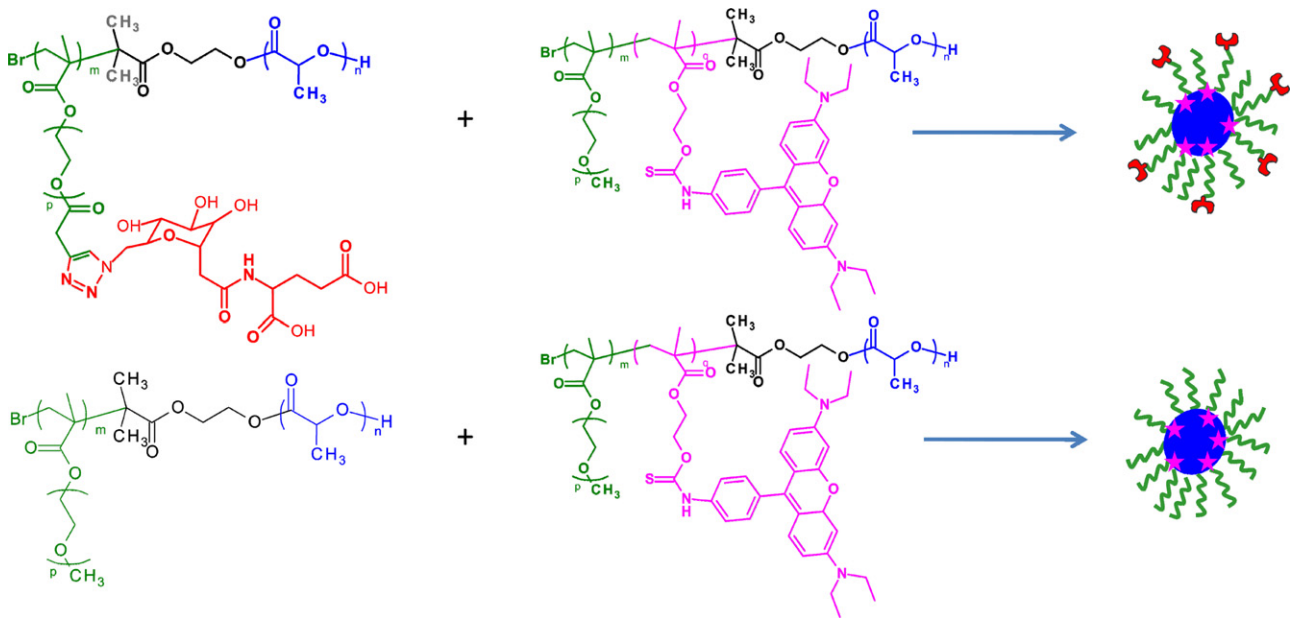

**Fig. 3.** Composition of the two types of nanoparticles prepared for this study.

expression was maximal after 4 h of activation (Bevilacqua et al., 1989).

High fluorescence could be observed in the level of the membrane of TNF-α-activated HUVECs (Fig. 5, upper panels) while a very weak fluorescence was detected on cells that were not pretreated with the pro-inflammatory agent (Fig. 5, lower panels). The lipophilic dye PKH67 was used to label the cell membrane and thus help to localize the E-selectin staining. This dye did not remain in the plasma membrane but also stained the membranes of intracellular structures. However, it allowed the cell contours to be visualized and did not interfere with the interpretation of E-selectin localization.

### 3.7. Nanoparticle association with HUVECs

The association of nanoparticles with stimulated and non-stimulated HUVECs was observed by laser scanning confocal microscope and quantified by measuring cell-associated fluorescence by spectrofluorimetry.

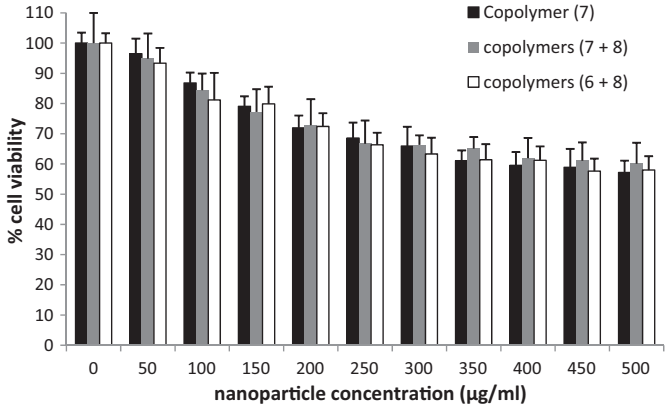


**Fig. 4.** HUVEC cell viability determination by the MTT assay after incubation with 0–500 μg/ml of different kinds of nanoparticles for 48 h. NP without rhodamine (black columns), NP-Rhod (gray columns) and NP-ligand-Rhod (white columns). Mean ± SD ($n > 5$).

Cells were incubated with nanoparticles for different times (30 min, 2 h and 21 h). Fig. 6 shows confocal micrographs of the cell monolayers incubated with nanoparticles for 21 h, The fluorescence of TNF-α-activated cells incubated with ligand-bearing nanoparticles was significantly higher than that observed with bare nanoparticles (Fig. 6a and b), indicating a predominantly selective uptake mediated by E-selectin. Moreover, the fluorescence was mainly distributed throughout the cytoplasm, as bright red spots. Cells incubated with fluorescently labeled bare nanoparticles displayed only very weak fluorescence that could be attributed to low non specific uptake of the particles. The nuclear area remained non fluorescent in all cases.

Some cell-associated fluorescence was also observed when ligand-bearing nanoparticles were incubated with non activated cells (Fig. 6c).

In order to quantify the association of nanoparticles with HUVECs, we measured the cell-associated fluorescence after different times of incubation with nanoparticles.

As shown in Fig. 7, the association of ligand-bearing nanoparticles with TNF-α-activated HUVECs was higher than that of bare nanoparticles or that of targeted nanoparticles added to unstimulated HUVECs. For example, after 2 h of incubation with ligand-bearing nanoparticles the cellular fluorescence was about 6 times higher than that of cells incubated with bare nanoparticles and 3 times higher than that of non activated cells incubated with ligand-bearing nanoparticles. Association of ligand-bearing nanoparticles with non activated cells is the sum of non specific association and the specific association due to the basal level of E-selectin expression, but this association is still many times lower than the one with activated cell. These results are in agreement with the observations by confocal microscopy. The level of ligand-bearing nanoparticle association with stimulated cells incubated at 4 °C was greatly reduced compared to 37 °C for all incubation times, indicating energy-dependent endocytosis of the functionalized nanoparticles.

In order to confirm the specific interaction between E-selectin and its ligand, a monoclonal antibody able to block the E-selectin receptor was used. When the antibody was applied to the cells prior to incubation with ligand-bearing nanoparticles, the cell-associated fluorescence was reduced by about 65% (results not

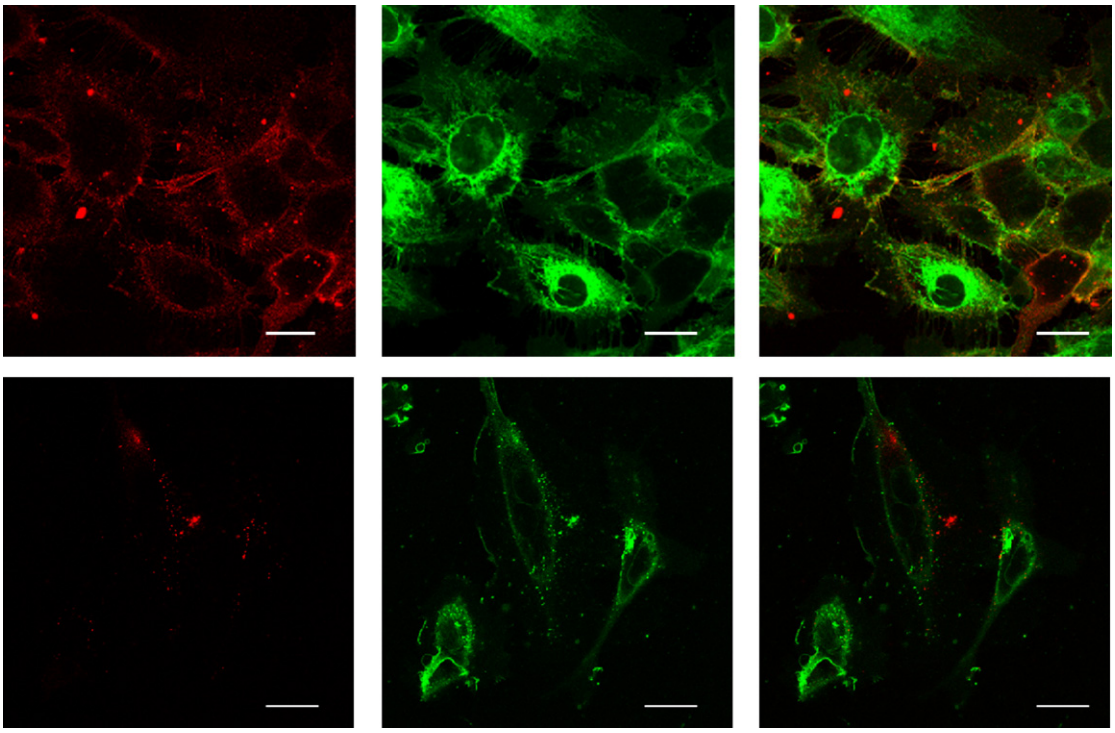

**Fig. 5.** Fluorescence imaging of activated HUVECs (lower panels) and non activated ones (upper panels). The red channel shows E-selectin localization. The green channel shows cellular lipids stained with FITC-PKH67.

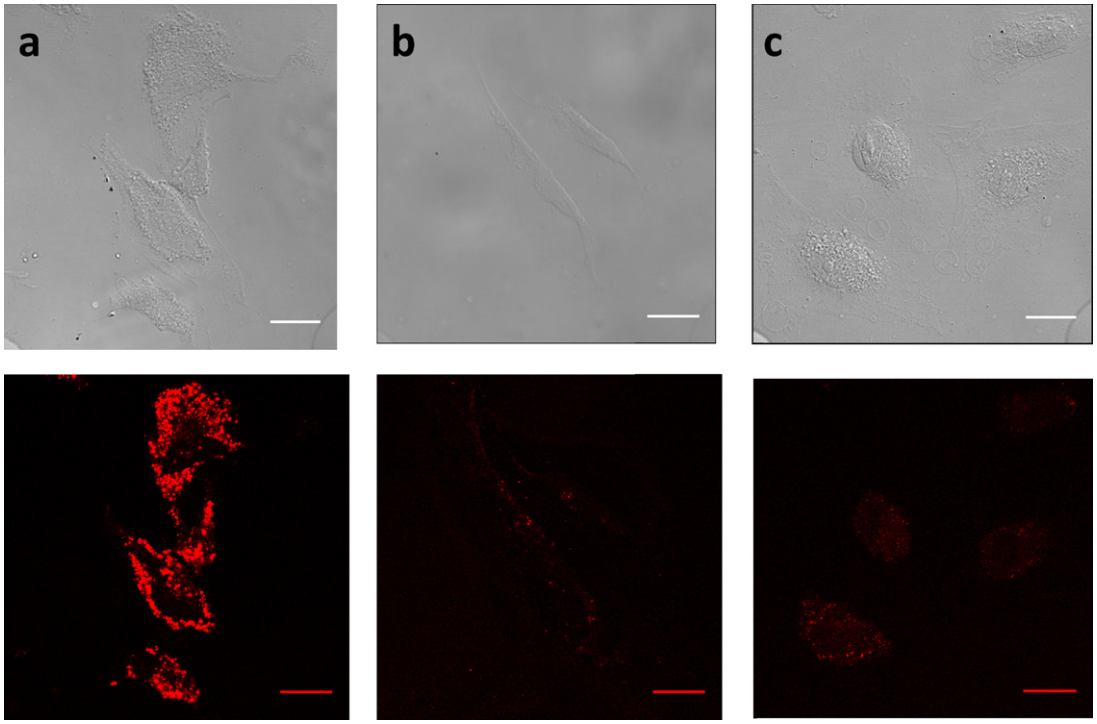


**Fig. 6.** Fluorescence imaging of nanoparticles incubated for 21 h with HUVECs under different conditions. Activated cells with ligand-bearing nanoparticles (left panels), activated cells with bare nanoparticles (middle panels) and non-activated cells with ligand nanoparticles (right panels). Differential contrast images (upper panels); red fluorescent channel (lower panels).

shown). From this result we can conclude that nanoparticles enter cells mainly through E-selectin-mediated uptake but that this is not the only mechanism of interaction.

## 4. Discussion

The vascular endothelium is a promising target for colloidal drug delivery systems since these are one of the first cell types in contact with these systems when they are administered by the intravenous route. Among the surface molecules expressed on endothelial cells, E-selectin is an attractive candidate for targeting to treat inflammation (Everts et al., 2002; Kok et al., 2002) and inhibit tumor metastasis (Stahn et al., 1998; Zeisig et al., 2004), as well as for in vivo imaging (Barber et al., 2004; Garrood et al., 2009; Jamar et al., 1995; Tsuruta et al., 2009).

Since up-regulation of this receptor as a result of tissue damage facilitates the recruitment of circulating leukocytes, we hypothesized that nanocarriers functionalized with an analog of SLEx would allow the carriers to accumulate in these regions.

It has been found that the six functional groups required for E-selectin binding are the 2-, 3- and 4-OH groups of fucose, the 4- and 6-OH groups of galactose and the $CO_2$-group of NeuAc (Wang and Wong, 1996). Hence libraries of different SLEx analogs have been proposed, including mono, bi, tri or tetrasaccharide-based structures (Kaila and Thomas, 2002; Simanek et al., 1998). These molecules would also be very useful as recognition elements to functionalize drug delivery systems that could carry cargo such as anti-inflammatory drugs, immunomodulators, anti-cancer drugs or imaging agents. Among these analogs of sialyl Lewis, we have chosen a mannose-based SLEx analog (Man-glu) developed by Wong et al. (Wong et al., 1997). This molecule has been successfully used as a recognition element connected directly to nanoparticles surface without a spacer (Banquy et al., 2008). In this study, the authors showed by docking experiments that the hydroxyl group at the 6-O position of the mannose is not essential for E-selectin-ligand binding; hence this hydroxyl could be used to connect the molecule to another structure such as a macromolecular chain of a drug delivery system. Based on these findings we chose to use this validated ligand to evaluate the efficiency of our macromolecular construction.

In a previous report we demonstrated that nanoparticles prepared from an amphiphilic copolymer with a similar structure to the one used here (glucose at the extremity of a hydrophilic PEG chain) can adopt an appropriate conformation in water where the sugar moieties are present on the surface and accessible to interact with a neighboring protein. In the present work we used the same strategy of synthesis to conjugate the Man-glu ligand to a PEG chain bearing a methacrylic monomer (PEGMA), so that the PEG chain would become a spacer, both allowing better molecular recognition and rendering the nanoparticle surface hydrophilic.

Click reaction between the azide- and acetylene-derivatized precursors could be carried out under mild conditions in a highly specific way with a good yield without affecting the methacrylate double bond. A combination of ATRP and ROP using a single bifunctional initiator allowed us to construct a well-defined amphiphilic block polymer. Conditions were modified to polymerize the Man-glu-Bz-conjugated monomer. Both types of polymerization were carried out with good yields and deprotection of benzyl groups was successfully achieved.

In this way, a functionalized copolymer, a non functionalized copolymer and a fluorescent copolymer with homologous structures were synthesized. Mixtures with different ratios of these copolymers can be used to prepare nanoparticles with varying surface ligand density, and varying fluorescence intensities. The use of copolymers with pre-conjugated ligand allows the ligand density

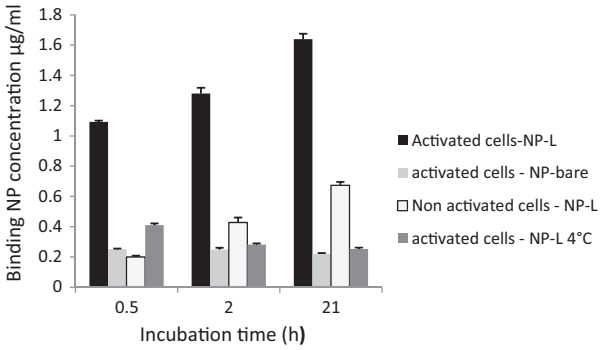


**Fig. 7.** Nanoparticle association with HUVEC under different conditions, measured by spectrofluorimetry as described in Materials and Methods. Mean ± SD ($n = 3$).

on the nanoparticle surface to be controlled, which is more difficult when methods of post-functionalization of pre-formed nanoparticles are used.

Man-glu-OH-functionalized nanoparticles did not have a large impact on the viability of endothelial cells over a large range of nanoparticle concentrations, suggesting that they could be safely administered by the IV route.

Endothelial cells have only low expression of E-selectin in normal physiological condition, but this expression is strongly up-regulated by factors such as TNF-α, IL-1 and LPS. Therefore, this receptor is an interesting target to direct drug delivery systems to damaged tissues.

Functionalized nanoparticles, in contrast to the non functionalized ones, were effectively internalized by HUVECs and this cell association was enhanced upon activation of the cells with TNF-α. This result confirms the specific binding properties of these nanoparticles and their potential as a drug targeting system. 65% of association was inhibited by pretreatment with anti-E-selectin antibody. These results suggest that our nanoparticles enter cells mainly by an E-selectin-mediated route. In fact, the ligand used in this work may also interact with P-selectin (Banquy et al., 2008) which was not blocked by the specific anti E-selectin antibody. The nanoparticles used here were negatively charged and it has been reported that negatively charged carriers can limit nonspecific adsorption with endothelial cells that are also negatively charged (Hirai et al., 2007, 2010), which could explain the low uptake of non functionalized nanoparticles.

These findings suggest that this type of system could have the double advantage of limiting immune cell adhesion by occupying their receptors and by concentrating an encapsulated drug in sites where the receptor is highly expressed.

## 5. Conclusion

Leukocyte-endothelial cell adhesion mechanisms were exploited to target biodegradable nanoparticles. We have used macromolecular chemistry techniques to construct a well-defined amphiphilic block polymer that was successfully used to prepare spherical nanoparticles using a simple nanoprecipitation method without any surfactant. These nanoparticles did not have a large impact on endothelial cell viability.

Coupling of a SLEx analog onto the surface of nanoparticles allowed efficient targeting of human endothelial cells overexpressing E-selectin with subsequent internalization by the cells.

These results suggest that such targeting systems could have the double action of inhibiting leukocyte infiltration into tissues beneath activated endothelium (since the receptor would be already occupied by particles) and being able to concentrate a drug encapsulated within these particles within the targeted tissue.

The system we propose here is a platform with flexible properties that can be summarized as follows: (i) the density of the ligand covalently fixed with the copolymer backbone can be modulated using different ratios of sugar-modified/non-modified monomers; (ii) the molecular weight of each polymer block can be fine-tuned to requirements using controlled polymerization methods and a well defined ratio monomer/initiator ratio; (iii) the chemical composition of the hydrophobic block could be modified using other cyclic monomers (i.e. $\varepsilon$-caprolactone, glycolide or derivatives of malic acid) that can be polymerized by ROP; (iv) the density of the PEG chains can be modified by the control of methacrylate block size within the ATRP; (v) many other potential ligands could be coupled using the efficient method of click chemistry after attachment of an azide group In order to target E-selectin or other molecular targets.

The next steps will be to evaluate interaction of these nanoparticles in vitro with serum proteins as an indicator of their ability to avoid uptake by the reticuloendothelial system. Their loading with an anti-inflammatory drug and their in vivo fate after intravenous administration will also be evaluated.

## Acknowledgments

The authors wish to thank Dr. Didier Desmaele (UMR CNRS 8076 Université Paris-Sud 11, France) for help in the deprotection of benzyl groups and Dr. Catherine Le Visage (Inserm U698 for supplying HUVECs). This work was supported by CNRS (programme: INTERFACE Physique-Chimie Biologie: aide à la prise de risque).

## Appendix A. Supplementary data

Supplementary data associated with this article can be found, in the online version, at doi:10.1016/j.ijpharm.2012.01.029.

## References

Adams, D.H., Hubscher, S.G., Fisher, N.C., Williams, A., Robinson, M., 1996. Expression of E-selectin and E-selectin ligands in human liver inflammation. Hepatology 24, 533–538.

Ali, M.M., Stover, H.D.H., 2004. Well-defined amphiphilic thermosensitive copolymers based on poly(ethylene glycol monomethacrylate) and methyl methacrylate prepared by atom transfer radical polymerization. Macromolecules 37, 5219–5227.

Asgeirsdottir, S.A., Zwiers, P.J., Morselt, H.W., Moorlag, H.E., Bakker, H.I., Heeringa, P., Kok, J.W., Kallenberg, C.G.M., Molema, G., Kamps, J.A.A.M., 2008. Inhibition of proinflammatory genes in anti-GBM glomerulonephritis by targeted dexamethasone-loaded AbEsel liposomes. Am. J. Physiol. Renal Physiol. 294, F554–F561.

Banquy, X., Leclair G, Rabanel, J.-M., Argaw, A., Bouchard J.-F., Hildgen, P., Giasson, S., 2008. Selectins ligand decorated drug carriers for activated endothelial cell targeting. Bioconjug. Chem. 19, 2030–2039.

Barber, P.A., Foniok, T., Kirk, D., Buchan, A.M., Laurent, S., Boutry, S., Muller, R.N., Hoyte, L., Tomanek, B., Tuor, U.I., 2004. MR molecular imaging of early endothelial activation in focal ischemia. Ann. Neurol. 56, 116–120.

Bendas, G., Krause, A., Bakowsky, U., Vogel, J., Rothe, U., 1999. Targetability of novel immunoliposomes prepared by a new antibody conjugation technique. Int. J. Pharm. 181, 79–93.

Bevilacqua, M.P., Stengelin, S., Gimbrone Jr., M.A., Seed, B., 1989. Endothelial leukocyte adhesion molecule 1: an inducible receptor for neutrophils related to complement regulatory proteins and lectins. Science 243, 1160–1165.

Brambilla, D., Nicolas, J., Le Droumaguet, B., Andrieux, K., Marsaud, V., Couraud, P.-O., Couvreur, P., 2010. Design of fluorescently tagged poly(alkyl cyanoacrylate) nanoparticles for human brain endothelial cell imaging. Chem. Commun. 46, 2602–2604.

Brigger, I., Dubernet, C., Couvreur, P., 2002. Nanoparticles in cancer therapy and diagnosis. Adv. Drug Deliv. Rev. 54, 631–651.

Chauvierre, C., Labarre, D., Couvreur, P., Vauthier, C., 2003. Novel polysaccharide-decorated poly(isobutyl cyanoacrylate) nanoparticles. Pharm. Res. 20, 1786–1793.

Everts, M., Kok, R.J., Asgeirsdottir, S.A., Melgert, B.N., Moolenaar, T.J., Koning, G.A., van Luyn, M.J., Meijer, D.K., Molema, G., 2002. Selective intracellular delivery of dexamethasone into activated endothelial cells using an E-selectin-directed immunoconjugate. J. Immunol. 168, 883–889.

Everts, M., Koning, G.A., Kok, R.J., Ásgeirsdóttir, S.A., Vestweber, D., Meijer, D.K.F., Storm, G., Molema, G., 2003. In vitro cellular handling and in vivo targeting of E-Selectin-directed immunoconjugates and immunoliposomes used for drug delivery to inflamed endothelium. Pharm. Res. 20, 64–72.

Garrood, T., Blades, M., Haskard, D.O., Mather, S., Pitzalis, C., 2009. A novel model for the pre-clinical imaging of inflamed human synovial vasculature. Rheumatology (Oxford) 48, 926–931.

Gref, R., Luck, M., Quellec, P., Marchand, M., Dellacherie, E., Harnisch, S., Blunk, T., Muller, R.H., 2000. 'Stealth' corona-core nanoparticles surface modified by polyethylene glycol (PEG): influences of the corona (PEG chain length and surface density) and of the core composition on phagocytic uptake and plasma protein adsorption. Colloids Surf. B: Biointerfaces 18, 301–313.

Gref, R., Minamitake, Y., Peracchia, M.T., Domb, A., Trubetskoy, V., Torchilin, V., Langer, R., 1997. Poly(ethylene glycol)-coated nanospheres: potential carriers for intravenous drug administration. Pharm. Biotechnol. 10, 167–198.

Gref, R., Quellec, P., Sanchez, A., Calvo, P., Dellacherie, E., Alonso, M.J., 2001. Development and characterization of CyA-loaded poly(lactic acid)-poly(ethylene glycol)PEG micro- and nanoparticles. Comparison with conventional PLA particulate carriers. Eur. J. Pharm. Biopharm. 51, 111–118.

Hartmuth, C.K., Finn, M.G., Barry Sharpless, K., 2001. Click chemistry: diverse chemical function from a few good reactions. Angew. Chem. Int. Ed. 40, 2004–2021.

Hashida, N., Ohguro, N., Yamazaki, N., Arakawa, Y., Oiki, E., Mashimo, H., Kurokawa, N., Tano, Y., 2008. High-efficacy site-directed drug delivery system using sialyl-Lewis X conjugated liposome. Exp. Eye Res. 86, 138–149.

Hirai, M., Minematsu, H., Hiramatsu, Y., Kitagawa, H., Otani, T., Iwashita, S., Kudoh, T., Chen, L., Li, Y., Okada, M., Salomon, D.S., Igarashi, K., Chikuma, M., Seno, M., 2010. Novel and simple loading procedure of cisplatin into liposomes and targeting tumor endothelial cells. Int. J. Pharm. 391, 274–283.

Hirai, M., Minematsu, H., Kondo, N., Oie, K., Igarashi, K., Yamazaki, N., 2007. Accumulation of liposome with Sialyl Lewis X to inflammation and tumor region: application to in vivo bio-imaging. Biochem. Biophys. Res. Commun. 353, 553–558.

Jamar, F., Chapman, P.T., Harrison, A.A., Binns, R.M., Haskard, D.O., Peters, A.M., 1995. Inflammatory arthritis: imaging of endothelial cell activation with an indium-111-labeled F(ab')2 fragment of anti-E-selectin monoclonal antibody. Radiology 194, 843–850.

Jubeli, E., Moine, L., Barratt, G., 2010. Synthesis, characterization, and molecular recognition of sugar-functionalized nanoparticles prepared by a combination of ROP, ATRP, and click chemistry. J. Polym. Sci. Part A: Polym. Chem. 48, 3178–3187.

Kaila, N., Thomas, B.E.t., 2002. Design and synthesis of sialyl Lewis(x) mimics as E- and P-selectin inhibitors. Med. Res. Rev. 22, 566–601.

Kang, H.W., Josephson, L., Petrovsky, A., Weissleder, R., Bogdanov, A., 2002a. Magnetic resonance imaging of inducible E-Selectin expression in human endothelial cell culture. Bioconjug. Chem. 13, 122–127.

Kang, H.W., Weissleder, R., Bogdanov Jr., A., 2002b. Targeting of MPEG-protected polyamino acid carrier to human E-selectin in vitro. Amino Acids 23, 301–308.

Kiriyama, K., Ye, C., 1995. E-selectin expression in serum and tissue correlates with distant metastasis of colorectal cancer. Nippon Rinsho 53, 1760–1764.

Kok, R.J., Everts, M., Asgeirsdottir, S.A., Meijer, D.K., Molema, G., 2002. Cellular handling of a dexamethasone-anti-E-selectin immunoconjugate by activated endothelial cells: comparison with free dexamethasone. Pharm. Res. 19, 1730–1735.

Kriegsmann, J., Keyszer, G.M., Geiler, T., Lagoo, A.S., Lagoo-Deenadayalan, S., Gay, R.E., Gay, S., 1995. Expression of E-selectin messenger RNA and protein in rheumatoid arthritis. Arthritis Rheum. 38, 750–754.

Lee, Y.C., Lee, R.T., 1995. Carbohydrate-protein interactions: basis of glycobiology. Acc. Chem. Res. 28, 321–327.

Lundquist, J.J., Toone, E.J., 2002. The cluster glycoside effect. Chem. Rev. 102, 555–578.

Mayer, B., Spatz, H., Funke, I., Johnson, J.P., Schildberg, F.W., 1998. De novo expression of the cell adhesion molecule E-selectin on gastric cancer endothelium. Langenbecks Arch. Surg. 383, 81–86.

Minaguchi, J., Oohashi, T., Inagawa, K., Ohtsuka, A., Ninomiya, Y., 2008. Transvascular accumulation of Sialyl Lewis X conjugated liposome in inflamed joints of collagen antibody-induced arthritic (CAIA) mice. Arch. Histol. Cytol. 71, 195–203.

Montgomery, K.F., Osborn, L., Hession, C., Tizard, R., Goff, D., Vassallo, C., Tarr, P.I., Bomsztyk, K., Lobb, R., Harlan, J.M., et al., 1991. Activation of endothelial-leukocyte adhesion molecule 1 (ELAM-1) gene transcription. Proc. Natl. Acad. Sci. U.S.A. 88, 6523–6527.

Myrset, A.H., Fjerdingstad, H.B., Bendiksen, R., Arbo, B.E., Bjerke, R.M., Johansen, J.H., Kulseth, M.A., Skurtveit, R., 2011. Design and characterization of targeted ultrasound microbubbles for diagnostic use. Ultrasound Med. Biol. 37, 136–150.

Nguyen, M., Corless, C.L., Kraling, B.M., Tran, C., Atha, T., Bischoff, J., Barsky, S.H., 1997. Vascular expression of E-selectin is increased in estrogen-receptor-negative breast cancer: a role for tumor-cell-secreted interleukin-1 alpha. Am. J. Pathol. 150, 1307–1314.

Passirani, C., Barratt, G., Devissaguet, J.P., Labarre, D., 1998. Long-circulating nanoparticles bearing heparin or dextran covalently bound to poly(methyl methacrylate). Pharm. Res. 15, 1046–1050.

Pattillo, C., Venegas, B., Donelson, F., Del Valle, L., Knight, L., Chong, P., Kiani, M., 2009. Radiation-guided targeting of combretastatin encapsulated immunoliposomes to mammary tumors. Pharm. Res. 26, 1093–1100.

Phillips, M.L., Nudelman, E., Gaeta, F.C., Perez, M., Singhal, A.K., Hakomori, S., Paulson, J.C., 1990. ELAM-1 mediates cell adhesion by recognition of a carbohydrate ligand, sialyl-Lex. Science 250, 1130–1132.

Renkonen, J., Makitie, A., Paavonen, T., Renkonen, R., 1999. Sialyl-Lewis(x/a)-decorated selectin ligands in head and neck tumours. J. Cancer Res. Clin. Oncol. 125, 569–576.
Shamay, Y., Paulin, D., Ashkenasy, G., David, A., 2009. Multivalent display of quinic acid based ligands for targeting E-selectin expressing cells. J. Med. Chem. 52, 5906–5915.
Simanek, E.E., McGarvey, G.J., Jablonowski, J.A., Wong, C.H., 1998. ChemInform Abstract: selectin – carbohydrate interactions from natural ligands to designed mimics. ChemInform 29.
Stahn, R., Grittner, C., Zeisig, R., Karsten, U., Felix, S.B., Wenzel, K., 2001. Sialyl Lewis(x)-liposomes as vehicles for site-directed, E-selectin-mediated drug transfer into activated endothelial cells. Cell. Mol. Life Sci. 58, 141–147.
Stahn, R., Schafer, H., Kernchen, F., Schreiber, J., 1998. Multivalent sialyl Lewis x ligands of definite structures as inhibitors of E-selectin mediated cell adhesion. Glycobiology 8, 311–319.
Stella, B., Marsaud, V., Arpicco, S., Geraud, G., Cattel, L., Couvreur, P., Renoir, J.M., 2007. Biological characterization of folic acid-conjugated poly(H2NPEGCA-co-HDCA) nanoparticles in cellular models. J. Drug Target. 15, 146–153.
Tsuruta, W., Tsurushima, H., Yamamoto, T., Suzuki, K., Yamazaki, N., Matsumura, A., 2009. Application of liposomes incorporating doxorubicin with sialyl Lewis X to prevent stenosis after rat carotid artery injury. Biomaterials 30, 118–125.
van Kasteren, S.I., Campbell, S.J., Serres, S., Anthony, D.C., Sibson, N.R., Davis, B.G., 2009. Glyconanoparticles allow pre-symptomatic in vivo imaging of brain disease. Proc. Natl. Acad. Sci. U.S.A. 106, 18–23.
von Asmuth, E.J., Smeets, E.F., Ginsel, L.A., Onderwater, J.J., Leeuwenberg, J.F., Buurman, W.A., 1992. Evidence for endocytosis of E-selectin in human endothelial cells. Eur. J. Immunol. 22, 2519–2526.
Walz, G., Aruffo, A., Kolanus, W., Bevilacqua, M., Seed, B., 1990. Recognition by ELAM-1 of the sialyl-Lex determinant on myeloid and tumor cells. Science 250, 1132–1135.
Wang, J., Liu, W., Tu, Q., Song, N., Zhang, Y., Nie, N., 2011. Folate-decorated hybrid polymeric nanoparticles for chemically and physically combined paclitaxel loading and targeted delivery. Biomacromolecules 12, 228–234.
Wang, R., Wong, C.-H., 1996. Synthesis of sialyl Lewis X mimetics: use of O-[alpha]-fucosyl-(1R, 2R)-2-aminocyclohexanol as core structure. Tetrahedron Lett. 37, 5427–5430.
Weitz-Schmidt, G., Stokmaier, D., Scheel, G., Nifant'ev, N.E., Tuzikov, A.B., Bovin, N.V., 1996. An E-selectin binding assay based on a polyacrylamide-type glycoconjugate. Anal. Biochem. 238, 184–190.
Wikaningrum, R., Highton, J., Parker, A., Coleman, M., Hessian, P.A., Roberts-Thompson, P.J., Ahern, M.J., Smith, M.D., 1998. Pathogenic mechanisms in the rheumatoid nodule: comparison of proinflammatory cytokine production and cell adhesion molecule expression in rheumatoid nodules and synovial membranes from the same patient. Arthritis Rheum. 41, 1783–1797.
Wolf, F.F., Friedemann, N., Frey, H., 2009. Poly(lactide)-block-Poly(HEMA) block copolymers: an orthogonal one-pot combination of ROP and ATRP, using a bifunctional initiator. Macromolecules 42, 5622–5628.
Wong, C.-H., Moris-Varas, F., Hung, S.-C., Marron, T.G., Lin, C.-C., Gong, K.W., Weitz-Schmidt, G., 1997. Small molecules as structural and functional mimics of sialyl Lewis X tetrasaccharide in selectin inhibition: a remarkable enhancement of inhibition by additional negative charge and/or hydrophobic group. J. Am. Chem. Soc. 119, 8152–8158.
Zeisig, R., Stahn, R., Wenzel, K., Behrens, D., Fichtner, I., 2004. Effect of sialyl Lewis X-glycoliposomes on the inhibition of E-selectin-mediated tumour cell adhesion in vitro. Biochim. Biophys. Acta 1660, 31–40.
Zhang, N., Chittasupho, C., Duangrat, C., Siahaan, T.J., Berkland, C., 2008. PLGA nanoparticle – peptide conjugate effectively targets intercellular cell-adhesion molecule-1. Bioconjug. Chem. 19, 145–152.